Biochemical Engineering Journal 90 (2014) 224–233

Contents lists available at ScienceDirect

Biochemical Engineering Journal

journal homepage: www.elsevier.com/locate/bej

The role of volumetric power input in the growth, morphology, and production of a recombinant glycoprotein by *Streptomyces lividans* in shake flasks

Luz D. Marín-Palacio[a,b], Ramsés A. Gamboa-Suasnavart[a], Norma A. Valdez-Cruz[c], Luis Servín-González[c], Ma. Soledad Córdova-Aguilar[d], Enrique Soto[d], Wolf Klöckner[e], Jochen Büchs[e], Mauricio A. Trujillo-Roldán[a,*]

[a] *Unidad de Bioprocesos, Departamento de Biología Molecular y Biotecnología, Instituto de Investigaciones Biomédicas, Universidad Nacional Autónoma de México, AP. 70228, CP. 0.4510, México, D.F., México*
[b] *Departamento de Ingeniería de Procesos, Universidad EAFIT. Medellín, Colombia*
[c] *Departamento de Biología Molecular y Biotecnología, Instituto de Investigaciones Biomédicas, Universidad Nacional Autónoma de México, AP. 70228, CP. 04510, México, D.F., México*
[d] *Centro de Ciencias Aplicadas y Desarrollo Tecnológico, Universidad Nacional Autónoma de México, CP 04510, México, D.F., México*
[e] *AVT–Biochemical Engineering, RWTH Aachen University, Worringer Weg 1, Aachen 52074, Germany*

ARTICLE INFO

Article history:
Received 1 February 2014
Received in revised form 12 May 2014
Accepted 12 June 2014
Available online 19 June 2014

Keywords:
Shaken bioreactors
Morphology
Orbital shaking
Power dissipation
Suspension rheology
Recombinant glycoproteins

ABSTRACT

The impact of flask geometry on *Streptomyces lividans* growth and morphology, production and *O*-mannosylation of a recombinant *O*-glycoprotein (APA from *Mycobacterium tuberculosis*) was described and associated to the evolution of the volumetric power input (P/V) in three shake flask geometries. During the exponential growth, the highest P/V was found in baffled flasks (BF) with 0.51 kW/m^3, followed by coiled flasks (CF) with 0.44 kW/m^3 and normal Erlenmeyer flasks (NF) with 0.20 kW/m^3 (flasks volume of 250 mL, filling with 50 mL and agitated at 150 rpm). During the stationary phase, P/V decreased 20% in BF and CF, but increased two times in NF, surely due to changes in mycelial morphology and its effects on rheology. Also, NF cultures were carried out at a filling volume and agitation of 15 mL, 150 rpm (15 mL-NF), and 25 mL, 168 rpm (25 mL-NF), in order to raise P/V closely to the values obtained in CF. However, different growth, morphology and recombinant protein productivity were obtained. These data indicate that P/V is not a definitive parameter that can determine bacteria growth and morphology, not even glycoprotein production. But it can be proposed that the oxygen transfer in the center of the pellets and hydromechanical stress might be the more relevant parameters than P/V.

1. Introduction

Bacteria of the genus *Streptomyces* are widely used to produce a large range of secondary metabolites including antimicrobial, antifungal, antihelmintic and antitumor agents, as well as herbicides, pigments and other bioactive compounds [1,2]. Also, some strains as *S. lividans* are commonly used as hosts for the expression of heterologous proteins [3–7]. *Streptomyces* are prokaryotes with similar aspects to filamentous fungi, both are dispersed in the form of spores and its growth is branching hyphae that form a vegetative mycelium [8–11]. Specifically, in submerged cultures *S. lividans* presents a filamentous morphology that may be branched and non-branched hyphae, clumped and pelleted [9,11]. Few attempts to understand a possible relation between morphology, growth and recombinant protein production have been reported [3,12,13]. Van Wezel et al. [13] described the successful morphological engineering of *S. coelicolor* and *S. lividans* through a controlled expression of the morphogene *ssgA*, leading to the improvement of growth by the fragmentation of the mycelial clumps resulting in increased growth rates for *S. lividans* of almost 45%, and the production of recombinant tyrosinase increased 2.5 times [13]. By using fluorescence microscopy and viability staining, Manteca et al. [14] reported that compartmentalized hyphae started to form pellets by radial growth of *S. coelicolor* A3(2), and in the center of the pellets a relatively quick cell death can be detected [14].

In various mycelial bacterial and fungal cultures it is known that the morphology of the culture largely depends on the hydrodynamic conditions, as well as on aeration and on culture

---

* Corresponding author. Tel.: +52 55 56229192; fax: +52 55 56223369.
E-mail address: maurotru@gmail.com (M.A. Trujillo-Roldán).

http://dx.doi.org/10.1016/j.bej.2014.06.010
1369-703X/

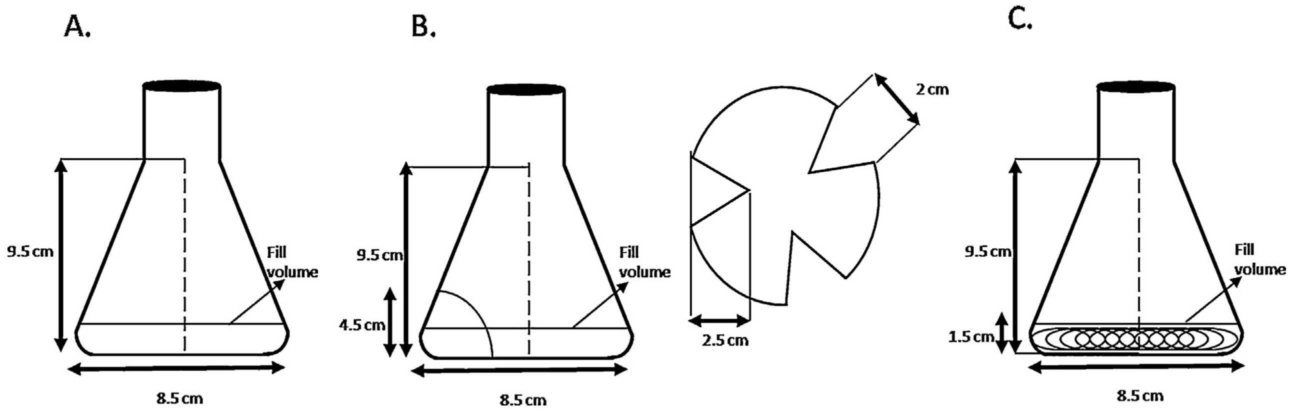

Fig. 1. Schematic diagrams of shake flasks used: (A) conventional Normal (NF); (B) baffled (BF); and (C) coiled shake flasks (CF). Diagrams taken with permission from Gamboa-Suasnavart et al. [3].

medium [15–19]. When using shake flasks, the effects on morphology, growth, and recombinant protein production in filamentous bacteria cannot be easily measured independently because the hydrodynamic and aeration phenomena are interrelated. However, shake flasks are the most commonly used bioreactors for cultures in literature, and deciding which flask design to use for filamentous cultures will be a key step in production or clone selection or in the inoculum train [20–22]. On the other hand, the power input per unit of liquid volume (P/V) has been intensively used for the characterization of macroscopic hydrodynamics in bioreactors, and lately in shake flask cultures [20,23–31].

The morphology of *S. lividans* depends on the hydromechanical stress and on the oxygenation of the culture as was demonstrated [3], both determined by the design of the shake flasks used to grow these bacteria (normal conventional, baffled and coiled shake flasks). Moreover, the shake flask design might be playing a role in the regulation of the productivity and *O*-glycosylation of a recombinant glycoprotein. The small and dispersed mycelia aggregates obtained in baffled (BF), and coiled (CF) shake flasks improve the production and increase the degree of *O*-mannosylation of the recombinant glycoprotein (up to five mannoses attached to the carboxy-terminal of the protein), in comparison with the large aggregates obtained in conventional normal (NF) shake flasks, with just two mannoses attached [3]. These differences in flask geometry, and therefore, the volumetric power input involved, might play a role in the changes shown in morphology, growth rate, and protein production in *S. lividans*, thereby suggesting that hydrodynamic effects may be involved in the performance of the microorganism. Moreover, mathematical models and experimental data of *S. coelicolor* cultures in bioreactors have been used to correlate volumetric power input and bacterial morphology [32,33]. With this model, a prediction of aggregate size of *S. lividans* in aerated bioreactor cultures based on the volumetric power input was made. These data were used to obtain a culture morphology in the bioreactor, similar to that previously reported in baffled/coiled shake flasks [33]. This successful scale-up strategy suggests that power input has an important influence on growth, morphology, and recombinant protein productivity of *S. lividans*. The aim of the current study was to find out the role of the volumetric power input by measuring the shear viscosity, the morphology and the development of P/V during the cultivation of a recombinant *S. lividans* strain, using the three shake flask configurations as previously reported [3]. Additionally, a comparison of *S. lividans* growth and morphology, rheology and recombinant protein production and its *O*-mannosylation profile was made, when NF cultures were carried out at a P/V value similar to the P/V values obtained in CF.

2. Materials and methods

2.1. Microorganisms, culture conditions and analytical determinations

Streptomyces lividans 66 strain 1326 was used in this work [34,35], and it was transformed with plasmid pIJ6021MT-45, which carries the *M. tuberculosis apa* gene (Rv1860), cloned under the thiostrepton-inducible P_{tipA} promoter [36]. Spores of *S. lividans* were maintained in 20% glycerol and kept at −20 °C, as a master bank. *S. lividans* spores were pregerminated in YT medium for 8 h at 37 °C, and 150 rpm [36]; the germinated spores were then washed and inoculated to shake flasks at an optical density of around 0.015 at 600 nm (Beckman DU730 spectrophotometer, USA).

The same shake flask designs previously used by Gamboa-Suasnavart et al. [3] were used (250 mL-flasks filled with 50 mL of medium). Normal Erlenmeyer flasks (NF), Baffled flasks (BF) with three baffles, 2.5 cm depth and 4.5 cm height, and coiled flasks (CF) with a stainless steel spring at the bottom, 1.3 cm diameter, 19 standard wire gauge (SWG), as is shown in Fig. 1. Luria–Bertani's medium supplemented with 50 μg/mL kanamycin and 34% w/v sucrose [36] was used. All cultures were carried out at 30 °C and 150 rpm for 72 h, with the addition of the inducer thiostrepton (10 μg/mL) at 16 h of culture. At least 20 shake flasks were used for each kinetic and two shake flasks were removed at each kinetic data point for biomass, protein and image analysis [3].

The biomass was evaluated by dry weight; 5 mL of culture were filtered through a 0.45 μm pore size membrane (Millipore, USA), and washed once with one volume of distilled water. The mycelium obtained was dried for 24 h in an oven at 55 °C, then placed for 2 h in a desiccator, and weighed afterwards [3].

The amount of protein in the culture supernatant was determined using the Bradford Method (Bio-Rad, Hercules, CA, USA). Electrophoresis in 12% polyacrylamide gels containing SDS and subsequent immunoblotting procedures were carried out as previously described [3]. For Western blots, 30 μg of total protein separated by SDS-PAGE (10%) were transferred to polyvinylidene difluoride membranes (Millipore). The membranes were incubated with 5% (w/v) skim milk in PBS containing Tween 20 (0.05% v/v) for 1 h, washed with PBS Tween 0.05%, and then incubated with primary antibody (mAb6A3) at a 1:1000 dilution overnight at 4 °C [3,36]. After three washes with PBS-Tween 20, the membranes were incubated with diluted peroxidase-conjugated anti-mouse IgG (Sigma–Aldrich, St. Louis, MO, USA) at a 1:2000 dilution for 2 h. After incubation, the blots were stained by using the Super-Signal West Pico Chemiluminescent Substrate (Pierce Chemical, Rockford, IL, USA) and images were taken using the theC-DiGit

Chemiluminescent Western Blot Scanner (Li-Cor, Lincoln, NE, USA).

2.2. Protein digestion and MALDI-TOF analysis

O-linked glycans at the C-terminal region of recombinant APA were characterized and the protein was purified and digested with LysC with the aim to produce at least eight peptides as previously reported [3]. The 45 and 47 kDa bands were excised from SDS-PAGE gels, washed with water, distained with ammonium bicarbonate buffer (100 mM, 50% methanol), dehydrated with acetonitrile (100%), and rehydrated with ammonium bicarbonate buffer (25 mM) containing the Lys-C enzyme (Roche) in 1:1000 dilution. Digestion was carried out overnight at 37 °C, and 20 µL of trifluoroacetic acid (TFA, 0.1% v/v) were added to stop the reaction. A concentration step was carried out to obtain 20 µL or less (Speed-Vac concentrator, Savant-Thermo). Masses were determined in a Bruker Microflex matrix-assisted laser desorption ionization time-of-flight instrument (Bruker Daltonics GmbH, Leipzig, Germany) equipped with a 20 Hz nitrogen laser at $l = 337$ nm. Spectra were recorded in reflector and/or linear positive mode for the mass range of 3800–6000 Da. 1.0 mL of sample solution was mixed with 5 mL of 30% acetonitrile, 70% water, 0.1% TFA, and saturated with α-cyano-4-hydroxycinnamic acid or sinapinic acid. Then, 1.0 µL of this solution was deposited onto the MALDI target, and allowed to dry at room temperature. At least three MALDI-TOF analyses were done at the end of each independent culture.

2.3. Measurements of power input

The development of the volumetric power input (P/V) was characterized on-line during *S. lividans* growth and APA production using the method previously described [24,25]. This method is based on torque measurements in the drive of the shaking machine with appropriate compensation of friction losses. Operating conditions for all cultures were: 150 rpm, 30 °C, flasks with nominal flask volume of 250 mL, filling volume of 50 mL (or as otherwise stated), and shaking diameter of 2.5 cm.

2.4. Rheological measurements

Rheological parameters of the culture broth were measured using 50 mm plate/plate geometry in a controlled stress Rheometer (Physica MCR 101 Modular Compact Rheometer, Anton Paar, Graz, Austria) at a constant temperature of 30 °C, using shear rates between 0.1 and 100 s^{-1}, and a gap between two plates of 1 mm. It was ascertained that the measurements were carried out within the sensitive range of the rheometer used and with the adequate time to reach the steady state in each shear rate. The dependency of the viscosity on the shear rate was described by the Ostwald–de Waele law:

$$\eta = K\gamma^{n-1} \tag{1}$$

where η is the apparent viscosity (m Pas), γ is the shear rate (s^{-1}), K is the consistency index (m Pas^n) and n is the flow behavior index (dimensionless).

2.5. Morphological measurements

The morphology of *S. lividans* in culture was measured as previously reported [3,33]. In brief, a sample of 20 µL of culture broth was fixed using a formalin solution (10%, v/v) in order to avoid the losses of the actual morphology, placed on a slide, and carefully covered with a cover slip. A minimum of 300 objects of each sample were analyzed for each determination. The image was captured with a digital camera Coolpix 4300 (Nikon, Tokyo Japan) mounted on a microscope (Nikon Optiphot-2, Tokyo Japan) that used a 4× magnification. Image analysis was performed with the software package ImageJ (National Institutes on Health, NIH, Bethesda, MD, USA) available on-line (http://imagej.nih.gov/ij/index.html).

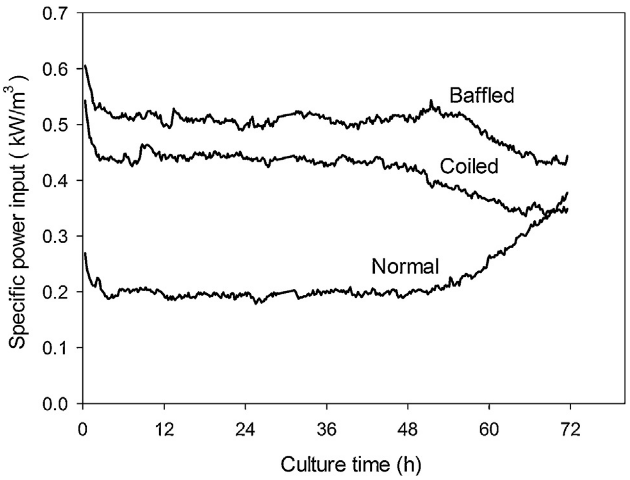

Fig. 2. Evolution of the volumetric power input during the cultivation of *Streptomyces lividans* producing rAPA from *M. tuberculosis*, in conventional normal (NF), baffled (BF), and coiled (CF) shake flasks with a nominal volume of 250 mL and 50 mL filling volume, incubated at a shaking frequency of 150 rpm and a shaking diameter of 25 mm.

3. Results and discussion

3.1. Measurements of power input in three different shake flasks designs

The development of P/V for cultures carried out in three different designs of 250 mL shake flasks (normal, baffled and coiled flasks, as is shown in Fig. 1) using a strain of *S. lividans* producing a recombinant protein is shown in Fig. 2. Maintaining the same agitation frequency of 150 rpm and the same filling volume of 50 mL, P/V remains substantially constant during the first 50 h, and the highest P/V was obtained for baffled flasks near 0.51 kW/m^3, followed by coiled flasks of roughly 0.44 kW/m^3, and then by conventional flasks of around 0.20 kW/m^3. Comparing the experimentally measured P/V in NF (0.20 kW/m^3), with the correlation proposed by Buchs (0.22 kW/m^3) [24,25] a good approximation was achieved with a difference of just 9%. However, in baffled flask, the correlation predictions from Peter et al. [20] a difference of 67% was found. This can be due to differences in baffles dimensions used in this experiment (25 mm deep and 45 mm high) and those used by Peter et al. [20] (14 mm deep and 35 mm high). Thereafter, the behavior of the P/V is not constant, it decreases to 0.44 kW/m^3 in BF and to 0.35 kW/m^3 in CF, respectively. In contrast, it increases to almost 0.38 kW/m^3 in NF. The initial values of P/V during the first 50 h are in agreement with values reported by Peter et al. [20], who proposed that the greater resistance to fluid flow in baffled flasks than in conventional normal ones generated greater P/V values [20]. By computational fluid dynamics (CFD) techniques, using volumetric average of turbulence parameters, Li et al. [27] found that each of these turbulence parameters in baffled flasks is greater than those in unbaffled flasks [27]. Velocity performance indicates that a greater velocity gradient is formed in baffled flasks. As a result, energy dissipation in baffled flasks is higher than that in unbaffled flasks. When the fluid hits the baffles, it splashes over the baffles, resulting in higher local velocity and energy dissipation, especially at the submerged corner between the baffle and the flask wall. This results in a better mixing and mass transfer capacity of baffled shake flasks [27].

On the other hand, to our knowledge, this is the first time that P/V was measured for any culture carried out in coiled flasks. P/V in CF has an intermediate value between conventional and baffled flasks (Fig. 2), suggesting that works as an obstacle that increase energy dissipation and promotes an increase in mass transfer coefficient as long as a good incorporation of the gas phase in the system, even though such contributions are smaller than in the baffled flask.

At the end of cultures carried out in NF, an increase in the medium apparent viscosity might be responsible for the increase of P/V [20,29]. An exponential increase in P/V, due to an increase in viscosity in cultures of alginate producing bacteria *Azotobacter vinelandii*, in normal conventional flasks has been found [29]. A maximum P/V of 1.4 kW/m^3, but a reduction at the end of cultures (1.2 kW/m^3) were due to a decrease in apparent viscosity, and the possible occurrence of the "out of phase" phenomena. Also, it has been demonstrated that at least at shaking diameter of 25 mm (shaking diameter employed in this study), cultures carried out in baffled flasks were out of phase [20]. Out of phase phenomenon is generated when parts of the liquid cannot follow the agitation motion, and therefore, remain at the bottom of the flask with little movement. This is associated with a reduction in power, a reduction in mass transfer, and flow irreproducibility [25]. However, out of phase cannot be easily associated to the end of cultures in BF or CF (Fig. 2), and the rheological complexity of cultures might be related to these changes in P/V.

3.2. Biomass growth, morphology and rheology in three different shake flasks designs

The highest biomass production was obtained in BF (5.6 ± 0.2 g/L), and CF (5.2 ± 0.1 g/L), which occurred at the maximum volumetric power input (0.51 and 0.44 kW/m^3, respectively), while at P/V of 0.20 kW/m^3 obtained in NF, the final biomass concentration was 2.1 ± 1.2 g/L (Fig. 3A). Moreover, the specific growth rate (μ) was significantly different in CF (0.14 ± 0.01 h^{-1}), BF (0.10 ± 0.01 h^{-1}), and NF (0.08 ± 0.01 h^{-1}) flasks. These results are in agreement with those reported by Gamboa-Suasnavart et al. [3] in terms of the specific growth rate, which has been previously reported in the range of 0.08–0.14 h^{-1} for the same shake flasks geometries [3]. However, there are differences in the final biomass concentrations obtained in this work (Fig. 3A) and those reported previously by other authors [3], where no significant differences were reported among BF, CF and NF (with an average of 3.3 ± 0.2 g/L). This differences in biomass growth can be attributed to differences in the inoculum size, as previously reported for *S. coelicolor* A3(2), where the low density inoculum (10^5 spores/mL) grew at a lower specific growth rate, reaching lower biomass than cultures with high density inoculum (10^7 spores/mL) [37]. Similar behavior was reported for *S. pristinaespiralis* where P/V positively affects the biomass concentration and the concentration of pristamycins, but they also are affected by the mass transfer coefficient k_La [21–23]. Moreover, it should be noted that in all the experiments carried out in this work, we used the same transformed strain of *S. lividans* and the same master bank.

A lag phase could be observed during the first 12 h of culture in all cases. However, in NF two stages in the exponential phase was observed. This second growth phase in NF where consistent with those previously reported [19,37,38]. In *S. coelicolor* A3(2), two growth stages are seen: a first where compartmentalized mycelium (first mycelium) is obtained, which starts to die in the center of the pellet to lead the appearance of a multinucleated mycelium (second mycelium) that grows from the remaining viable hyphae [37]. This phenomena of two growth phases seem to be associated with low volumetric power input in combination with low inoculum size in *S. coelicolor* [32,37,39], *S. fradiae* [18,40], *S. noursei* [41], and *S. natalensis* [42].

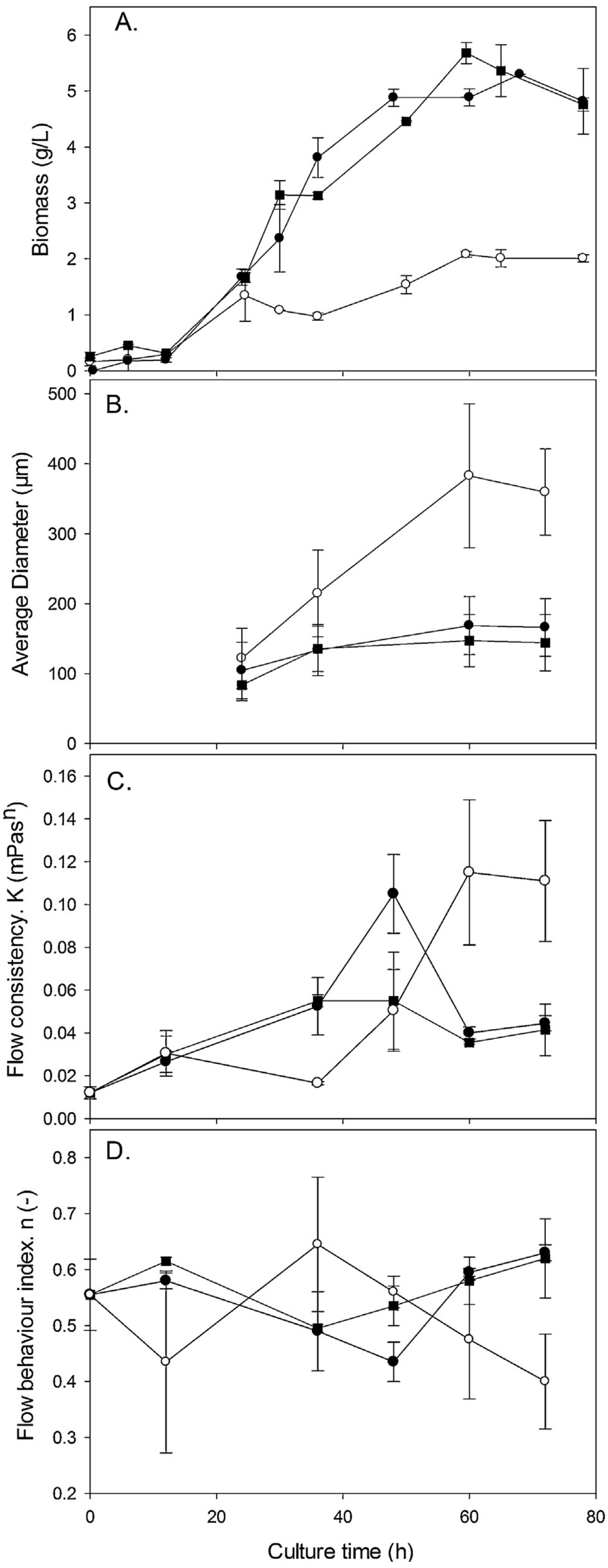

Fig. 3. (A) Kinetics of biomass growth of *S. lividans* producing rAPA from *M. tuberculosis*. (B) Average diameter and standard deviation of *S. lividans* pellets. (C) Evolution of the flow consistency index *K* (m Pas^n) and (D) flow behavior index *n* (–) of cultures in conventional normal (open dots); baffled (square); and coiled (closet dots) shake flasks with a filling volume 50 mL incubated at a shaking frequency of 150 rpm and shaking diameter of 25 mm.

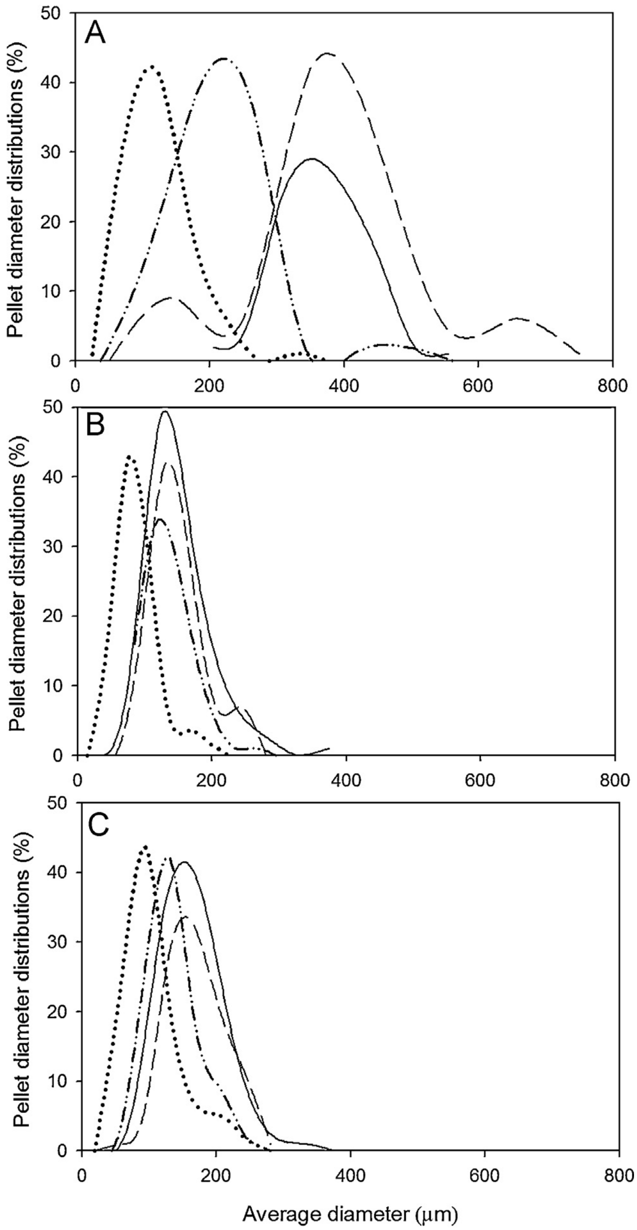

Fig. 4. *S. lividans* pellet diameter distributions in (A) conventional normal (NF); (B) baffled (BF); and (C) coiled (CF) shake flasks. Samples were taken at 24 h (dotted), 36 h (dash–dot–dot), 60 h (long-dash), and 78 h (solid) of culture.

According to previously reported data for 100 mL shake flasks [31], a P/V of around 0.1–0.2 kW/m^3 was delivered to the cultures using conventional 100 mL shaking flasks with a working volume of 20 mL, incubated at 200 rpm (shaking diameter was not reported) [39], a value similar to that reported in this work for NF, that is almost 0.22 kW/m^3 during the first 45 h of culture (Fig. 2).

The kinetics of the pellet size for NF, BF and CF was followed by sampling cultures at 24, 36, 60, and 78 h of culture in triplicates, and analyzing at least a minimum of 300 objects per sample for each determination (Figs. 3B and 4). During the first hours of the cultivation, the average diameter of the pellets to the three design flask were approximately 100 μm. However, the pellet grows in size until it reaches a stable state, being higher in normal flasks. In NF, pellets increased up to an average pellet size of 370 ± 82 μm, but a wide range of diameters was obtained, including pellets of up to 700 μm (Fig. 4), while in BF and CF cultures, the obtained average diameter was up to 160 ± 40 μm, with a narrow distribution and approximately 60% smaller pellets in average than those obtained in NF. Significant differences are shown only at the end of cultivation time between CF and BF. This might be due to the flow patterns and velocity fields in these geometries that are different presenting greater heterogeneity in the intensity of turbulence in CF, which could to influence the greatest number of dispersed mycelium (Fig. S2 and Table S1 included in the supplementary data). Apart from that, the same trend as previously reported by Gamboa-Suasnavart et al. [3] was found in this work, with larger pellets in NF and no significant differences between BF and CF. This difference in pellet sizes between both works, might be attributed to differences in the inoculum size, as previously reported for *S. coelicolor* [37], indicating that while the power input is responsible for morphological changes, the inoculum size also plays an important role.

At a P/V of 0.20 kW/m^3, the pellets were observed as internally compact and fluffy in the peripheral region (Fig. 5). Meanwhile, the pellets obtained at 0.51 and 0.44 kW/m^3 (BF and CF) had an oval shape and were less compact (Fig. 5). These changes in the pellet size for the three flask geometries could be explained by differences in the energy dissipation rates due to the P/V delivered to cultures. BF and CF had higher P/V (0.51 and 0.44 kW/m^3, respectively), compared to conventional flasks (0.20 kW/m^3).

The rheological behavior of the bacterial cultures of *S. lividans* for the three flask geometries in terms of the Ostwald-de Waele model (The complete shear flow result is included as supplementary data in the manuscript, Fig. S1), the evolution of the flow consistency index (K), and the flow behavior index (n) are shown in Fig. 3C and D. At the end of the cultivation, the flow consistency index increases three times (0.111 ± 0.024 m Pas^n) in NF cultures when compared to BF and CF cultures (0.042 ± 0.009 and 0.045 ± 0.003 m Pas^n, respectively), but the behavior index decreases by 33% in NF (0.40 ± 0.06) in comparison with BF and CF (0.62 ± 0.05 and 0.63 ± 0.01, respectively). This change in the rheological characteristics of the cultures seems to be related to the change in the P/V behavior found between 56 and 58 h of culture (Fig. 2). The increase in P/V at the end of NF cultures or the decrease in CF and BF, might be related with the increase in NF or decrease in CF and BF of the consistency index. As also, with the decrease in NF and the increase in CF and BF in the behavior index. This indicates an increase in NF or a decrease in CF and BF in the apparent viscosity of the culture, and also an increase in NF but a decrease in CF and BF in the pseudoplastic behavior of cultures. The pseudoplastic changes may surely be associated with the changes in morphological sizes at late stages of the cultures in NF. Similar behaviors were found for mycelial cultures of *S. clavuligerus* [43], *S. pristinaespiralis* [23], and *S. olindensis* [10,44]. We could not realize whether these rheological changes are due to morphology or composition of the culture medium modifications, but these rheological changes concur with P/V behavior at the end of cultures. Furthermore, we observed dispersed mycelium and this was not quantified, and we thought that this can also be affected volumetric power (through rheological modifications).

3.3. Recombinant APA production and O-mannosylation in three different shake flasks designs

Significant differences were found in the recombinant APA protein produced, similar to the data previously reported [3]. A lower productivity was found in NF (lanes C50, Fig. 8) compare with CF (lane R, Fig. 8). Likewise, specific host released proteins at the end of cultures follow the same trend, with lower amounts of proteins in NF, and higher amounts in BF and CF [3].

There are four putative sites of *O*-mannosylation in APA from *Mycobacterium tuberculosis*, one of which is located at the carboxy-terminal region [45,46]. The carbohydrate composition of this site was determined by mass spectrometry and up to six mannose

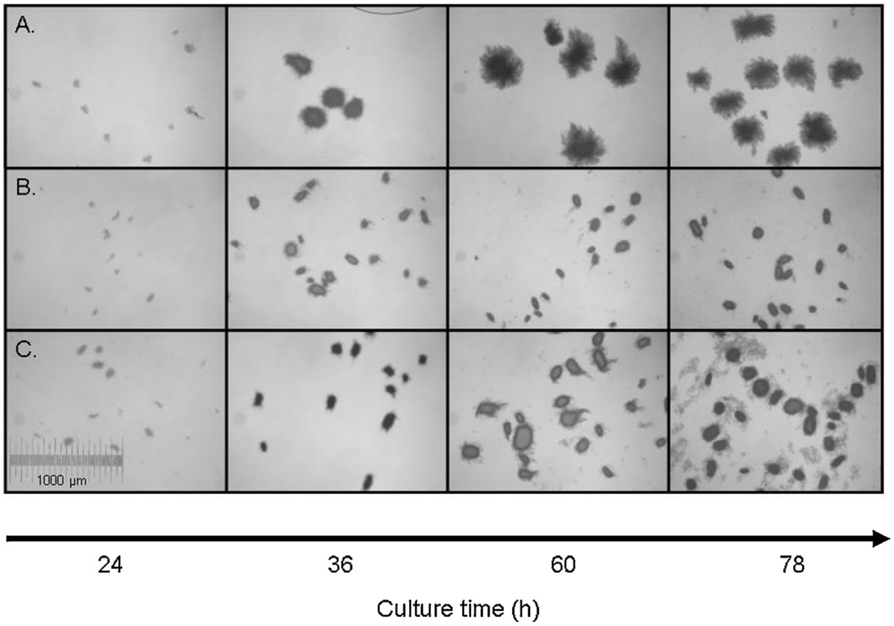

Fig. 5. Representative mycelial kinetic morphology of *S. lividans* cultured in (A) conventional normal (NF); (B) baffled (BF); and (C) coiled shake flasks (CF). Samples were taken at 24, 36, 60, and 78 h of culture. (Bar indicates 1000 μm, 4× magnification).

residues were found in NF and CF. These data are different to those previously reported in our group [3], where up to two mannose residues in cultures carried out in NF, and up to five mannose residues were determined in CF and BF.

The differences in the number of mannose residues found in the carboxy-terminal of recombinant APA in NF in this work, and the just two mannose residues previously reported [3], are most probably due to the four times difference in pellet size found. This suggests that also oxygen supply was a limiting step in the inside of large pellets, as those previously reported [3], surely limiting post-translational modifications such as *O*-mannosylation of the recombinant proteins. Also, as previously discussed, unavoidable differences in growth/morphology can be attributed to differences in inoculum size [21–23,37]. As a consequence of the changes in pellet size between works, a different critical oxygen concentration to ensure a properly diffuse into the aggregate is expected. According to the correlation proposed [15], 0.8 mg/L are required to suffice the diffusion in pellets of 370 ± 80 μm diameter (this work), even with the maximal diameter of 700 μm, 1.2 mg/L are needed. Contrastingly, 14.28 mg/L in 1.57 ± 0.41 mm [3] are needed. The solubility of oxygen in pure water at 25 °C is 8.5 mg/L, approximately. Therefore, we suggest that in 1.57 ± 0.41 mm aggregates there is oxygen limitation but in the pellets obtained in this work there is not.

The hypothesis of a threshold value of aggregate size to achieve a certain number of mannose residues, al least in the carboxy-terminal of the APA protein, as a result of an oxygen limitation, could be confirmed by displaying a systematic study. This can be done in order to demonstrate that P/V and oxygen transfer rate, in conjunction with mycelium inoculum size, has an important role in triggering the multinucleated mycelium appearance in *S. lividans*, as the corresponding aggregate size distribution associated to this. This has to be done in cultures in bioreactors, where mass and momentum transfer phenomena can be studied separately [47]. It was reported that the center of mycelium pellets contains inactive cells, due to a rapid consumption of substrates (nutrients and/or oxygen) within the kernel of the pellets [37]. However, It has been found that mass transfer concerns were negligible in *S. lividans* growth, when pellets reach diameters around 2 mm, at least in terms of oxygen transfer [48]. Nevertheless, this threshold value of aggregate size can be smaller to affect post-translational modifications of proteins, as in the case of NF aggregates reported in previous works [3]. It can be proposed that not only inoculum size, but also low agitation/aeration may be playing a specific role in determining the two growth phase phenomena, mainly at low power input (as in NF), where transient growth arrests can be triggered [37].

3.4. Biomass growth, morphology and rheology replicating the P/V from coiled flasks in normal flasks

In order to discern the specific role of P/V in the determination on growth and morphology of *S. lividans*, two different approaches were taken to increase the power input up to those values found in coiled flasks, but this time in conventional normal Erlenmeyer flasks (NF). The first approach was setting the shaking frequency to 150 rpm and decreasing filling volume of 50 mL–15 mL (15 mL-NF). These operating conditions were obtained using modified Newton number [24,25]. The second approach was done by setting the filling volume to 25 mL using modified Newton number equation [24], which gave us the result of 168 rpm (25 mL-NF) as the shaking frequency (Fig. 6). Even at the beginning of cultures the power input was similar in 15 mL-NF and 25 mL-NF to data obtained in coiled flasks, the decrease in P/V found at the end of cultures in CF, was not found in the normal shake flasks where P/V was increased (Fig. 6). For 15 mL-NF and 25 mL-NF, P/V measurements were 0.44 and 0.47 kW/m^3 respectively (Fig. 6), when compared those data with the correlation prediction proposed by Buchs et al. [24,25] values of 0.51 and 0.49 kW/m^3 were obtained. This prediction just has a difference of 14.7 and 5.1% to experimental data.

In cultures carried out in 15 mL-NF, a final concentration of biomass of 4.7 ± 0.3 g/L was obtained with a specific growth rate (μ) of 0.15 ± 0.01 h^{-1}. However, for those cultures carried out with a working volume of 25 mL and 168 rpm, a final biomass concentration of just 2.5 ± 0.4 g/L with a μ of 0.10 ± 0.03 h^{-1} was obtained (Fig. 7A). In 15 mL-NF no significant difference in maximum biomass was found, and μ when compared with CF, showed a lag phase and a small growth become visible in the first 36 h of culture. In contrast, in 25 mL-NF no significant difference was found in maximum biomass and μ when compared with NF filled with 50 mL. In spite of a well-simulated volumetric power input

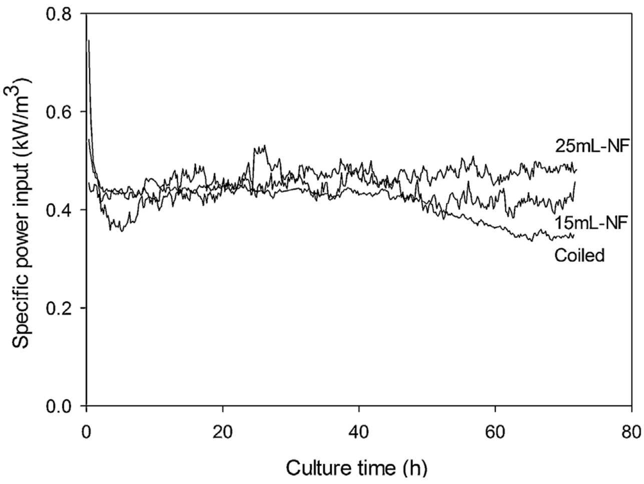

Fig. 6. Evolution of the volumetric power input during the cultivation of *S. lividans* producing rAPA from *M. tuberculosis*, in conventional normal (NF) shake flasks with a nominal volume of 250 mL at coiled flask equivalent P/V changing filling volume and agitation. 15 mL, 150 rpm (15 mL-NF), and 25 mL, 168 rpm (25 mL-NF). For comparison the P/V of a coiled flask (presented in Fig. 1) with a filling volume 50 mL incubated at a shaking frequency of 150 rpm and shaking diameter of 25 mm is included.

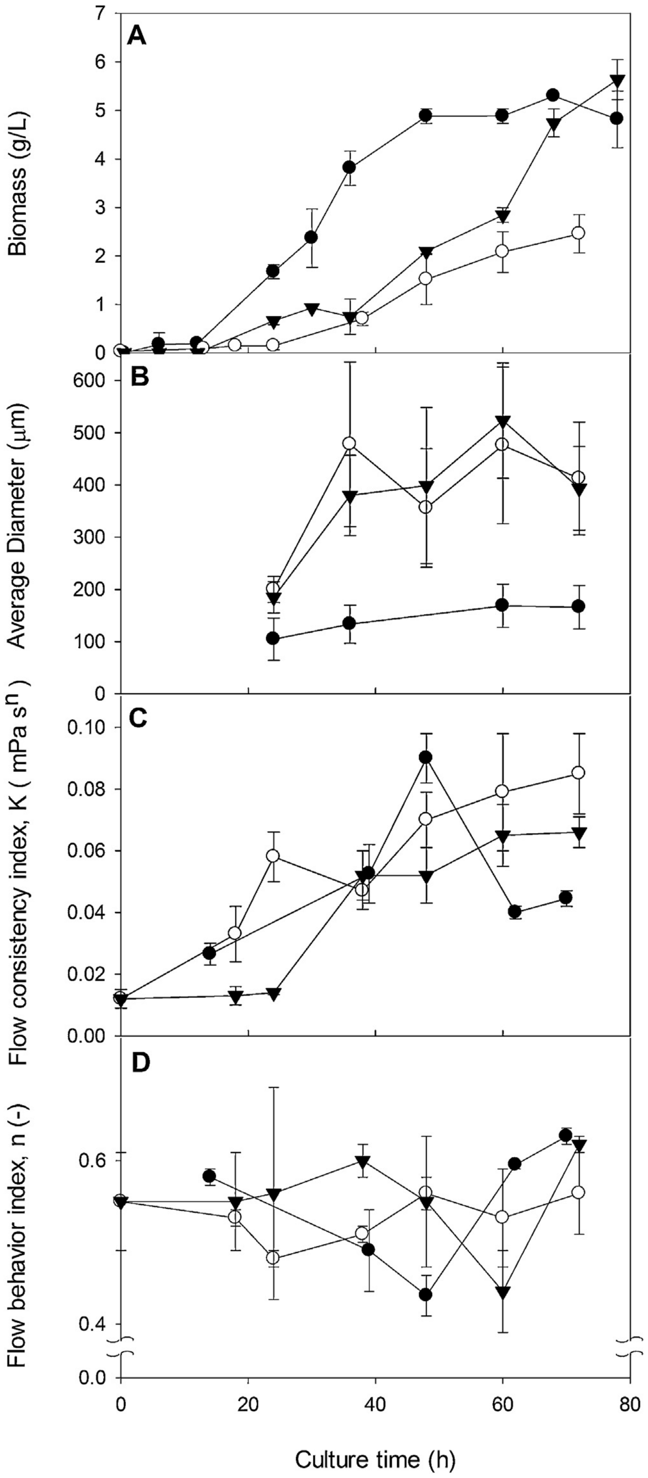

Fig. 7. (A) Kinetics of biomass growth of *S. lividans* producing rAPA from *M. tuberculosis*, in conventional normal flasks (NF) at equivalent P/V of coiled shake flasks. (B) Average diameter and standard deviation of *S. lividans* pellets. (C) Evolution of the flow consistency index *K* (m Pas^n) and (D) flow behavior index *n* (-)of cultures at equivalent P/V, with a changing filling volume and agitation frequency of 15 mL and 150 rpm (15 mL-NF, triangles), and 25 mL and 168 rpm (25 mL-NF, open dots). For comparison the data presented in Fig. 1 for coiled flasks are included (CF, closed dots) with a filling volume 50 mL incubated at a shaking frequency of 150 rpm and shaking diameter of 25 mm.

in 15 mL-NF and in 25 mL-NF, biomass growth results showed that this type of strategies to equate P/V were not adequate, at least for mycelial cultures. This is surely due to the differences in oxygen transfer rate (OTR) in NF, CF, 15 mL-NF and 25 mL-NF. The effect of the filling volume on OTR has been previously reported in other models as *Corynebacterium glutamicum* [49,50], *E. coli* [51], *Hansenula polymorpha* [52], *Pichia pastoris* [53] among others, as being also the effect of the type of shake flask on OTR [54]. In *S. pristinaespiralis* the effects of power dissipation on biomass growth were indirect, through the augmentation of oxygen transfer rates [22].

Aggregate diameters similar to NF (370 ± 80 μm) were obtained in 15 mL-NF and 25 mL-NF (412 ± 107 μm), and were higher than those in CF (160 ± 40 μm), as can be seen in Fig. 6B. These data indicate that not only P/V, as a global parameter in shake flasks, is playing an important role in *S. lividans* physiology, but also oxygen transfer rate and/or gradients of specific dissipation energy associated to shake flasks indentations in BF or springs in CF play that role. Computational fluid dynamics associated to particle image velocimetry might be important tools to resolve these inquiries [27,31].

The rheological behavior of the bacterial cultures of *S. lividans* for conventional normal flasks with a filling volume of 25 mL and 168 rpm (25 mL-NF) and 15 mL and 150 rpm (15 mL-NF) in terms of the Ostwald-de Waele model, the evolution of the flow consistency index (*K*) and the flow behavior index (*n*) are shown in Fig. 7C and D. At the end of the cultivation, the flow consistency index was 0.055 ± 0.004 m Pas^n for 15 mL-NF and 0.080 ± 0.013 m Pas^n for 25 mL-NF and the flow behavior index was 0.62 ± 0.007 for 15 mL-NF and 0.55 ± 0.049 for NF-25 mL. No significant differences were found with the rheological parameters obtained in CF.

3.5. Recombinant APA production and O-mannosylation replicating the P/V from coiled flasks in normal flasks

Interestingly, higher recombinant APA productivity was found in 15 mL-NF (45 ± 2% of total released proteins), no significant differences were obtained in 25 mL-NF (36 ± 3%), and coiled flasks (35.2%), and lower APA productivity was found in NF (25.2 ± 3%) (Fig. 8A). Also, this was corroborated by Western blots (Fig. 8B).

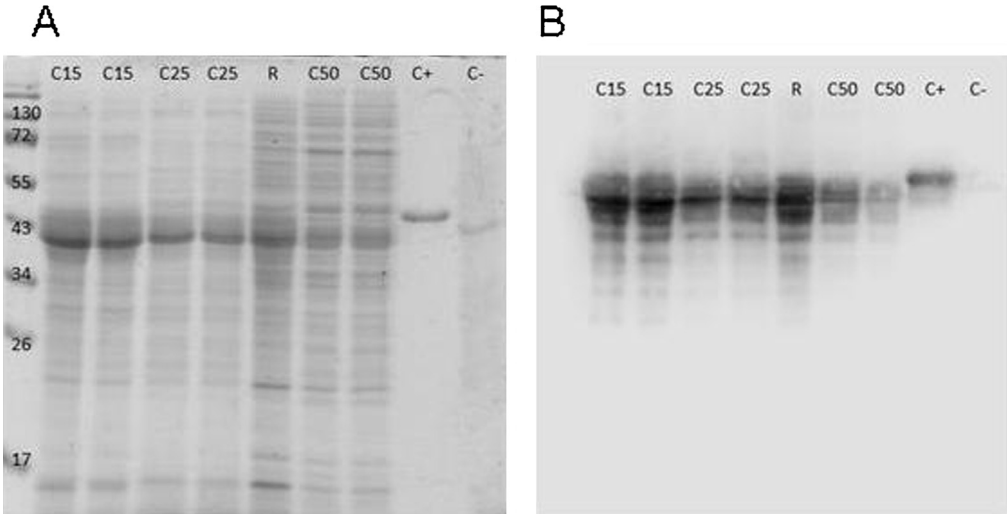

Fig. 8. (A) SDS-PAGE of total secreted proteins by *S. lividans* in the utilized shake flasks. (B) Western blot of rAPA production by *S. lividans* in the utilized shake flasks. Lane 1: page ruler. Lanes 2 and 3 (C15): two independent conventional normal flasks with a filling volume of 15 mL and 150 rpm (15 mL-NF). Lanes 4 and 5 (C25): two independent conventional normal flasks with a filling volume of 25 mL and 168 rpm (25 mL-NF). Lane 6 (R): coiled flasks. Lanes 7 and 8 (C50): two independent normal conventional shake flasks (NF). Lane 9: positive control, recombinant APA produced in bioreactor cultures of *E. coli*. Lane 10 (C−): negative control, *Streptomyces lividans* 66 strain 1326, without transformation.

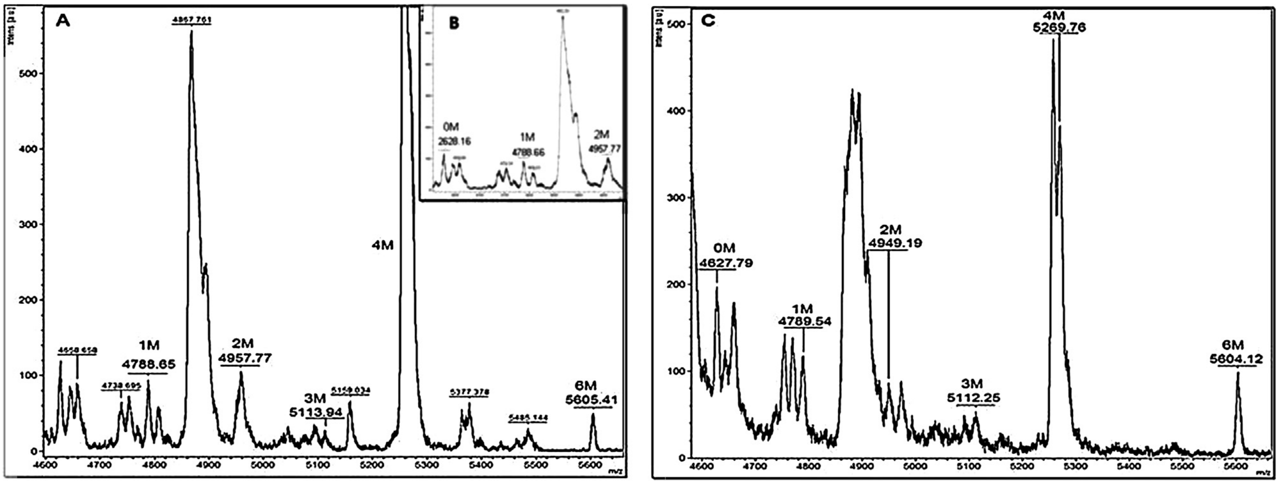

Fig. 9. MALDI-TOF analysis for the carboxy-terminal peptide of the recombinant APA protein by LysC digestion and obtained in (A) conventional normal flasks with a filling volume of 15 mL and 150 rpm (15 mL-NF) (B) the non *O*-glycoform with a molecular mass of 4628.16 Da in 15 mL-NF and (C) conventional normal flasks with a filling volume of 25 mL and 168 rpm (25 mL-NF). Numbers above each peak mean the number of mannose units linked to the peptide. At least three MALDI-TOF analyses were done at the end of each independent culture.

The positive control (APA protein produced in *E. coli*) was used as molecular weight reference in western blots (Fig. 8B), using the monoclonal antibody (mAb6A3) against the APA protein.

In other words, a significant effect on the specific heterologous protein productivity by increasing the volumetric power input (0.44 kW/m^3) in conventional flasks (15 mL-NF and 25 mL-NF), increases recombinant APA productivity, up to those obtained in coiled flasks (0.44 kW/m^3), although sizes of the cell aggregates are similar to those reported in conventional flasks (NF, 0.20 kW/m^3). On the other hand, the same *O*-mannosylation in the carboxy-terminal region and up to six mannose residues were found in 15 mL-NF and 25 mL-NF (Fig. 9). These results might support the idea that recombinant APA productivity is not being affected by size of the aggregate, but surely by the oxygen transfer rate inside the aggregate, through the increasing of the volumetric power input.

4. Conclusions

In this work, an approach has been developed to understand the role of the volumetric power input on the physiology of a recombinant strain of *S. lividans* producing the APA glycoprotein from *M. tuberculosis*, by using three shake flask designs. As it was previously suggested, the mass/momentum transfer is associated with the morphology, growth, APA production and *O*-mannosylation [3].

The specific recombinant APA productivity is probably not affected by the size of the *S. lividans* aggregates, but surely by the oxygen transfer inside them. The increase in OTR might be occurring through the increasing of the volumetric power input, as it can be seen in conventional flasks (15 mL-NF and 25 mL-NF), where volumetric power input was increased (0.44 kW/m^3) and although sizes of the cell aggregates are similar to those reported in conventional flasks (NF, 0.20 kW/m^3). Our data indicates that the role of

P/V, as a global parameter in *S. lividans* cultures in shake flasks, is not clearly defined as an important parameter to determine *S. lividans* growth, morphology, recombinant protein production, and its post-translational modifications (as it is the case of *O*-mannosylation of the carboxy-terminal peptide of APA).

Finally, the effect of the filling volume and shake flask glass composition on the OTR have been previously reported in other models [54]. However, to our knowledge no reports have been made on the geometry of the flasks. It would be attractive to study the OTR of filamentous bacterial cultures in order to determine whether this parameter has any role in the determination of growth and mycelial morphology.

Acknowledgements

This work was partially financed by Consejo Nacional de Ciencia y Tecnología (CONACyT 178528, CONACYT-INNOVAPYME 214404), and Programa de Apoyo a Proyectos de Investigación e Innovación Tecnológica, Universidad Nacional Autónoma de México (PAPIIT-UNAM IN-210013 and IN-209113). The primary antibody mAb6A3 was donated by Dra. Clara Espitia. LDMP thanks the scholarship Francisco José de Caldas from Colciencias-Colombia and EAFIT University (Colombia), for support her PhD studies at the Programa de Doctorado en Ciencias Bioquímicas, Universidad Nacional Autónoma de México. RAGS thanks the scholarship from CONACYT-México. We also thank Dr. Miguel Tapia Rodríguez for his technical assistance in image analysis and Ana Carmen Delgado for reviewing the English version of the manuscript.

Appendix A. Supplementary data

Supplementary material related to this article can be found, in the online version, at http://dx.doi.org/10.1016/j.bej.2014.06.010.

References

[1] A.K. Chaudhary, D. Dhakal, J.K. Sohng, An insight into the “-omics” based engineering of streptomycetes for secondary metabolite overproduction, Biomed. Res. Int. (2013) 968518.

[2] K.S. Hwang, H.U. Kim, P. Charusanti, B.O. Palsson, S.Y. Lee, Systems biology and biotechnology of Streptomyces species for the production of secondary metabolites, Biotechnol. Adv. (2013), http://dx.doi.org/10.1016/j.biotechadv.2013.10.008.

[3] R.A. Gamboa-Suasnavart, N.A. Valdez-Cruz, L.E. Cordova-Davalos, J.A. Martinez-Sotelo, L. Servin-Gonzalez, C. Espitia, M.A. Trujillo-Roldan, The *O*-mannosylation and production of recombinant APA (45/47 KDa) protein from *Mycobacterium tuberculosis* in *Streptomyces lividans* is affected by culture conditions in shake flasks, Microb. Cell Fact. 10 (2011) 110.

[4] L. Liu, H. Yang, H.D. Shin, J. Li, G. Du, J. Chen, Recent advances in recombinant protein expression by *Corynebacterium*, *Brevibacterium*, and *Streptomyces*: from transcription and translation regulation to secretion pathway selection, Appl. Microbiol. Biotechnol. 97 (2013) 9597–9608.

[5] E. Pimienta, J.C. Ayala, C. Rodriguez, A. Ramos, M.L. Van, C. Vallin, J. Anne, Recombinant production of *Streptococcus equisimilis* streptokinase by *Streptomyces lividans*, Microb. Cell Fact. 6 (2007) 20.

[6] C. Vallin, A. Ramos, E. Pimienta, C. Rodriguez, T. Hernandez, I. Hernandez, S.R. Del, G. Rosabal, M.L. Van, J. Anne, Streptomyces as host for recombinant production of *Mycobacterium tuberculosis* proteins, Tuberculosis (Edinb) 86 (2006) 198–202.

[7] K. Vrancken, J. Anne, Secretory production of recombinant proteins by *Streptomyces*, Future Microbiol. 4 (2009) 181–188.

[8] K. Flärdh, M.J. Buttne, *Streptomyces* morphogenetics: dissecting differentiation in a filamentous bacterium, Nat. Rev. Microbiol. 7 (2009) 36–49.

[9] J. Anne, B. Maldonado, I.J. Van, M.L. Van, K. Bernaerts, Recombinant protein production and *Streptomycetes*, J. Biotechnol. 158 (2012) 159–167.

[10] J. Anne, L. Van Mellaert, *Streptomyces lividans* as host for heterologous protein production, FEMS Microbiol. Lett. 114 (1993) 121–128.

[11] R. Giudici, C.R. Pamboukian, M.C. Facciotti, Morphologically structured model for antitumoral retamycin production during batch and fed-batch cultivations of *Streptomyces olindensis*, Biotechnol. Bioeng. 86 (2004) 414–424.

[12] G.P. van Wezel, M.J. van der, E. Taal, H. Koerten, B. Kraal, Effects of increased and deregulated expression of cell division genes on the morphology and on antibiotic production of streptomycetes, Antonie Van Leeuwenhoek 78 (2000) 269–276.

[13] G.P. van Wezel, P. Krabben, B.A. Traag, B.J. Keijser, R. Kerste, E. Vijgenboom, J.J. Heijnen, B. Kraal, Unlocking *Streptomyces* spp. for use as sustainable industrial production platforms by morphological engineering, Appl. Environ. Microbiol. 72 (2006) 5283–5288.

[14] A. Manteca, D. Claessen, C. Lopez-Iglesias, J. Sanchez, Aerial hyphae in surface cultures of *Streptomyces lividans* and *Streptomyces coelicolor* originate from viable segments surviving an early programmed cell death event, FEMS Microbiol. Lett. 274 (2007) 118–125.

[15] Y.Q. Cui, R.G. van der Lans, K.C. Luyben, Effects of dissolved oxygen tension and mechanical forces on fungal morphology in submerged fermentation, Biotechnol. Bioeng. 57 (1998) 409–419.

[16] L.F. Dobson, C.C. O’Cleirigh, D.G. O’Shea, The influence of morphology on geldanamycin production in submerged fermentations of *Streptomyces hygroscopicus* var. geldanus, Appl. Microbiol. Biotechnol. 79 (2008) 859–866.

[17] B.H. Junker, M. Hesse, B. Burgess, P. Masurekar, N. Connors, A. Seeley, Early phase process scale-up challenges for fungal and filamentous bacterial cultures, Appl. Biochem. Biotechnol. 119 (2004) 241–277.

[18] S. Tamura, Y. Park, M. Toriyama, M. Okabe, Change of mycelial morphology in tylosin production by batch culture of *Streptomyces fradiae* under various shear conditions, J. Ferment. Bioeng. 83 (1997) 523–528.

[19] P. Yin, Y.H. Wang, S.L. Zhang, J. Chu, Y.P. Zhuang, N. Chen, X.F. Li, Y.B. Wu, Effect of mycelial morphology on bioreactor performance and avermectin production of *Streptomyces avermitilis* in submerged cultivations, J. Chin. Inst. Chem. Eng. 39 (2008) 609–615.

[20] C.P. Peter, Y. Suzuki, J. Büchs, Hydromechanical stress in shake flasks: correlation for the maximum local energy dissipation rate, Biotechnol. Bioeng. 93 (2006) 1164–1176.

[21] N. Mehmood, E. Olmos, J.L. Goergen, F. Blanchard, D. Ullisch, W. Klöckner, J. Büchs, S. Delaunay, Oxygen supply controls the onset of pristinamycins production by *Streptomyces pristinaespiralis* in shaking flasks, Biotechnol. Bioeng. 108 (2011) 2151–2161.

[22] N. Mehmood, E. Olmos, J.L. Goergen, F. Blanchard, P. Marchal, W. Klöckner, J. Büchs, S. Delaunay, Decoupling of oxygen transfer and power dissipation for the study of the production of pristinamycins by *Streptomyces pristinaespiralis* in shaking flasks, Biochem. Eng. J. 68 (2012) 25–33.

[23] N. Mehmood, E. Olmos, P. Marchal, J.L. Goergen, S. Delaunay, Relation between pristinamycins production by *Streptomyces pristinaespiralis*, power dissipation and volumetric gas-liquid mass transfer coefficient, kLa, Process Biochem. 45 (2010) 1779–1786.

[24] J. Büchs, U. Maier, C. Milbradt, B. Zoels, Power consumption in shaking flasks on rotary shaking machines: I. Power consumption measurement in unbaffled flasks at low liquid viscosity, Biotechnol. Bioeng. 68 (2000) 589–593.

[25] J. Büchs, U. Maier, C. Milbradt, B. Zoels, Power consumption in shaking flasks on rotary shaking machines: II. Nondimensional description of specific power consumption and flow regimes in unbaffled flasks at elevated liquid viscosity, Biotechnol. Bioeng. 68 (2000) 594–601.

[26] J. Büchs, Introduction to advantages and problems of shaken cultures, Biochem. Eng. J. 7 (2001) 91–98.

[27] C. Li, J.Y. Xia, J. Chu, Y.H. Wang, Y.P. Zhuang, S.L. Zhang, CFD analysis of the turbulent flow in baffled shake flasks, Biochem. Eng. J. 70 (2013) 140–150.

[28] C. Peña, M. Millán, E. Galindo, Production of alginate by *Azotobacter vinelandii* in a stirred fermentor simulating the evolution of power input observed in shake flasks, Process Biochem. 43 (2008) 775–778.

[29] C. Peña, C.P. Peter, J. Büchs, E. Galindo, Evolution of the specific power consumption and oxygen transfer rate in alginate-producing cultures of *Azotobacter vinelandii* conducted in shake flasks, Biochem. Eng. J. 36 (2007) 73–80.

[30] C. Reyes, C. Peña, E. Galindo, Reproducing shake flasks performance in stirred fermentors: production of alginates by *Azotobacter vinelandii*, J. Biotechnol. 105 (2003) 189–198.

[31] H. Zhang, W. Williams-Dalson, E. Keshavarz-Moore, P.A. Shamlou, Computational-fluid-dynamics (CFD) analysis of mixing and gas–liquid mass transfer in shake flasks, Biotechnol. Appl. Biochem. 41 (2005) 1–8.

[32] A.J. Tough, J.I. Prosser, Experimental verification of a mathematical model for pelleted growth of *Streptomyces coelicolor* A3(2) in submerged batch culture, Microbiology 142 (1996) 639–648.

[33] R.A. Gamboa-Suasnavart, L.D. Marin-Palacio, J.A. Martinez-Sotelo, C. Espitia, L. ServÍn-González, N.A. Valdez-Cruz, M.A. Trujillo-Roldán, Scale-up from shake flasks to bioreactor, based on power input and *Streptomyces lividans* morphology, for the production of recombinant APA (45/47 kDa protein) from *Mycobacterium tuberculosis*, World J. Microbiol. Biotechnol. 29 (2013) 1421–1429.

[34] T. Kieser, M.T. Moss, J.W. Dale, D.A. Hopwood, Cloning and expression of *Mycobacterium bovis* BCG DNA in “*Streptomyces lividans*”, J. Bacteriol. 168 (1986) 72–80.

[35] T. Kieser, M.J. Bibb, M.J. Buttner, K.F. Chater, D.A. Hopwood, Practical *Streptomyces* Genetics, John Innes Foundation, Norwich Research Park, Colney, Norwich, United Kingdom, 2000.

[36] M. Lara, L. Servin-Gonzalez, M. Singh, C. Moreno, I. Cohen, M. Nimtz, C. Espitia, Expression, secretion, and glycosylation of the 45- and 47-kDa glycoprotein of *Mycobacterium tuberculosis* in *Streptomyces lividans*, Appl. Environ. Microbiol. 70 (2004) 679–685.

[37] A. Manteca, R. Alvarez, N. Salazar, P. Yague, J. Sanchez, Mycelium differentiation and antibiotic production in submerged cultures of *Streptomyces coelicolor*, Appl. Environ. Microbiol. 74 (2008) 3877–3886.

[38] B. Rioseras, M.T. Lopez-Garcia, P. Yague, J. Sanchez, A. Manteca, Mycelium differentiation and development of *Streptomyces coelicolor* in lab-scale

bioreactors: programmed cell death, differentiation, and lysis are closely linked to undecylprodigiosin and actinorhodin production, Bioresour. Technol. 151 (2014) 191–198.

[39] A. Manteca, J. Sanchez, *Streptomyces* development in colonies and soils, Appl. Environ. Microbiol. 75 (2009) 2920–2924.

[40] S. Khaliq, K. Akhtar, M. fzal Ghauri, R. Iqbal, A. Mukhtar Khalid, M. Muddassar, Change in colony morphology and kinetics of tylosin production after UV and gamma irradiation mutagenesis of *Streptomyces fradiae* NRRL-2702, Microbiol. Res. 164 (2009) 469–477.

[41] E. Jonsbu, M. McIntyre, J. Nielsen, The influence of carbon sources and morphology on nystatin production by *Streptomyces noursei*, J. Biotechnol. 95 (2002) 133–144.

[42] H.A. el-Enshasy, M.A. Farid, S. el-Sayed, Influence of inoculum type and cultivation conditions on natamycin production by *Streptomyces natalensis*, J. Basic Microbiol. 40 (2000) 333–342.

[43] E.R. Gouveia, A. Baptista-Neto, C.O. Hokka, J. Badino, Studies on the rheology and oxygen mass transfer in the clavulanic acid production by *Streptomyces clavuligerus*, Braz. J. Chem. Eng. 17 (2000) 827–834.

[44] C.R.D. Pamboukian, M.C.R. Facciotti, Rheological and morphological characterization of *Streptomyces olindensis* growing in batch and fed-batch fermentations, Braz. J. Chem. Eng. 22 (2005) 31–40.

[45] K. Dobos, K. Khoo, K. Swiderek, P. Brennan, J. Belisle, Definition of the full extent of glycosylation of the 45-kilodalton glycoprotein of *Mycobacterium tuberculosis*, J. Bacteriol. 178 (1996) 2498–2506.

[46] C. Horn, A. Namane, P. Pescher, M. Riviere, F. Romain, G. Puzo, O. Barzu, G. Marchal, Decreased capacity of recombinant 45/47-kDa molecules (Apa) of *Mycobacterium tuberculosis* to stimulate T lymphocyte responses related to changes in their mannosylation pattern, J. Biol. Chem. 274 (1999) 32023–32030.

[47] M.A. Trujillo-Roldán, S. Moreno, G. Espin, E. Galindo, The roles of oxygen and alginate-lyase in determining the molecular weight of alginate produced by *Azotobacter vinelandii*, Appl. Microbiol. Biotechnol. 63 (2004) 742–747.

[48] S.I. Yun, A.R. Yahya, M. Malten, D. Cossar, W.A. Anderson, J.M. Scharer, M. Moo-Young, Peptidases affecting recombinant protein production by *Streptomyces lividans*, Can. J. Microbiol. 47 (2001) 1137–1140.

[49] T. Anderlei, W. Zang, M. Papaspyrou, J. Büchs, Online respiration activity measurement (OTR, CTR RQ) in shake flasks, Biochem. Eng. J. 17 (2004) 187–194.

[50] H.F. Zimmermann, T. Anderlei, J. Büchs, M. Binder, Oxygen limitation is a pitfall during screening for industrial strains, Appl. Microbiol. Biotechnol. 72 (2006) 1157–1160.

[51] M. Losen, B. Frolich, M. Pohl, J. Büchs, Effect of oxygen limitation and medium composition on *Escherichia coli* fermentation in shake-flask cultures, Biotechnol. Prog. 20 (2004) 1062–1068.

[52] T. Anderlei, J. Büchs, Device for sterile online measurement of the oxygen transfer rate in shaking flasks, Biochem. Eng. J. 7 (2001) 157–162.

[53] U. Maier, M. Losen, J. Büchs, Advances in understanding and modeling the gas-liquid mass transfer in shake flasks, Biochem. Eng. J. 17 (2004) 155–167.

[54] U. Maier, J. Büchs, Characterisation of the gas-liquid mass transfer in shaking bioreactors, Biochem. Eng. J. 7 (2001) 99–106.